

Filling the voids in silicon single crystals by precipitation of Cu_3Si

Cheng-Yen Wen & Frans Spaepen*

Harvard School of Engineering and Applied Sciences, Cambridge, MA 02138 USA

This article presents a method to decorate all open volume defects in a silicon single crystal by Cu_3Si precipitation. Si single crystals are being used for the determination of Avogadro's number with sufficient accuracy (1 part in 10^8) to allow the establishment of a physical standard for the kilogram. The method described here can be used to certify that the open volume in such crystals is sufficiently small. The voids in this work were formed artificially by annealing He-implanted silicon wafers. Annealing after application of a copper nitrate solution to the surface followed by slow cooling produced Cu_3Si precipitates in the η' phase in the voids. To fill all the voids completely it proved necessary to coat the surfaces, after application of the nitrate, with a pure Cu layer as well. Slow cooling keeps the supersaturation of Cu small but sufficient to precipitate Cu into the voids. Formation of dislocation loops and stacking faults, often seen during Cu silicide precipitation in silicon after fast cooling, can be minimized. Other transition metals, such as Au, Ni, and Fe were found to be less suitable than Cu for filling voids.

Keywords: Silicon; Voids; Cu_3Si ; Precipitation; Avogadro

*Corresponding author. Email: spaepen@seas.harvard.edu

1 Introduction

Precipitation of transition and noble metals in silicon is of a great concern to the semiconductor device industry. Among these metals, Cu has been studied intensively since Dash used it to decorate dislocations in silicon crystals [1]. Precipitation of Cu in silicon proceeds by formation of Cu silicide either heterogeneously at lattice imperfections, such as dislocations [1–6], stacking faults [7, 8], and grain boundaries [9], or homogeneously in the silicon lattice [10, 11]. The crystal structure of the precipitates examined in the transmission electron microscope (TEM) was reported to be the η'' -Cu₃Si phase, in which the volume per Si atom is larger than in the silicon diamond cubic lattice [12]. Growth models of Cu₃Si precipitates were therefore proposed based on a strain relaxation mechanism [11, 13], such that Cu₃Si nucleates at lattice imperfections that serve as vacancy sources or reduce the lattice strain. In recent transition-metal gettering technology, Cu precipitation in silicon cavities was observed as a monolayer formed on the cavity wall [14] or as a crystalline silicide phase inside the cavity [15], depending on the nature, and hence the chemical potential of the Cu source.

During Si single crystal growth, by either the float-zone (FZ) or the Czochralski (Cz) method, equilibrium point defects are generated at the solid-liquid interface. Coalescence of these point defects during cooling leads to formation of various grown-in defects that depend on the growth parameters. In dislocation-free FZ Si crystals under fast growth conditions, voids are formed by aggregation of vacancies, as revealed by Cu decoration and X-ray topography [16]. The concentration of the voids was estimated to be $10^9/\text{cm}^3$. As the growth rate decreases, the major defects change to extrinsic dislocation loops. On the other hand, Cz Si crystals are usually grown under conditions that result in formation of voids. Several techniques have been used to observe voids and to quantify their concentration [17]. The precision of the concentration or size measurement, however, is still limited.

A need to certify the quality of a Si single crystal to a high degree arose in the project of determining Avogadro's number in order to redefine the standard for the kilogram [18]. The approach is based on the measurement of the density, molar mass and lattice parameter of a large FZ Si single crystal, perfect to 10 ppb; in other words: a void volume of less than $4.3 \times 10^{-3} \text{ mm}^3$ in 1 kg Si. In some measurements, however, a density deficit as large as 4 ppm has been observed [19]. A method more precise than those available for determining the void volume in a Si single crystal is necessary to certify the perfection of the Avogadro crystals to the required level of 10 ppb. To this end, a new method has been proposed [20], which consists of the following steps. Cu atoms are introduced into a Si crystal by annealing until the equilibrium concentration is reached. Cu diffuses fast in Si by an interstitial mechanism [21], so that the equilibrium solid solubility can be established in a short time. Subsequent cooling causes supersaturation of the Cu, which becomes the driving force for precipitation of Cu silicide in the voids. The interstitial Cu atoms that remain after precipitation are removed by out-diffusion at a lower temperature, with the sample surface serving as the sink for the Cu atoms [14]. After cleaning the surface, the entire sample - crystal with embedded Cu silicide precipitates in the voids - is dissolved in acid. The amounts of Cu and Si are then determined by an analytic method of requisite precision (e.g. inductively coupled plasma mass spectroscopy [22]). If the structure and composition of the precipitates is known, the total volume of the voids can be calculated.

The aim of this study is to establish a protocol for filling *all* voids in a Si sample as a first step in the implementation of this new method. Since the total number of Cu atoms can only *exceed* that in the precipitates in the voids (in solution, homogeneous precipitates, and other extended defects), the void volume calculated is an *upper limit*, which is a safe value for certifying the quality of the crystal for the Avogadro project. Since the grown-in voids in silicon crystals are small in size (around 100 nm or smaller) and number, it is difficult to use

such samples to study filling of the voids by TEM. Instead, artificial voids of size less than 100 nm were created by annealing He-implanted silicon wafers, in which the concentration and the location of the voids were well under control. A number of experimental parameters were varied and the degree of filling was checked until complete filling was achieved reliably and reproducibly. The dissolution rate of the precipitates was checked to ensure that no dissolution occurred under the condition of out-diffusion of the interstitial Cu. It has been reported that other fast diffusers such as Ni, Au, and Fe can also be trapped on the void walls in Si [23–25], so they are also candidates for decorating the voids. We also performed experiments with these elements and showed that Cu is uniquely suited for the purpose of the Avogadro project.

2 Experiments

Voids were created by implanting He at 30 keV to a dose of 2×10^{16} ions/cm² into n(phosphorus)-type (100) FZ silicon wafers at room temperature followed by 800°C annealing for 3 hours in flowing argon. The process of creating near-surface voids by the out-diffusion of He from bubbles formed by implantation is described by Griffioen *et al.* [26]. Under our conditions [14] stable voids at a concentration of 6.2×10^{10} /cm² are created. The voids are located in a 50 nm thick layer at 250 nm below the sample surface. Other silicon substrates were implanted with 2 MeV He to a dose of 3.6×10^{15} /cm² at room temperature. After the same thermal treatment voids formed a 100 nm thick layer at a depth of about 7 μ m; sometimes a line of voids perpendicular to the surface (parallel to the implantation beam) at a depth 3 to 10 μ m was also observed.

The samples with voids were etched in hydrofluoric acid to remove the surface oxide, and a 100 μ l drop of copper nitrate solution (1000 μ g/ml Cu in 5% HNO₃) was placed on the back side. It was found that a Cu capping layer on the sample surface was required to make

Cu precipitate in all the voids. Therefore, after the Cu nitrate solution was dried, a 100 nm Cu film was vapor deposited on all the surfaces of the samples before annealing. To test the precipitation behavior of the other transition metals, Ni, Au, and Fe, similar experimental procedures were used. Each metal was introduced from a solution source: 10000 $\mu\text{g}/\text{ml}$ Ni in 5% HNO_3 , 10000 $\mu\text{g}/\text{ml}$ Au in 10% HCl , and 2500 $\mu\text{g}/\text{ml}$ Fe in dilute HNO_3 .

Microstructural analysis of the precipitates was carried out in a field emission TEM, JEOL 2010F, operated at 200 kV. TEM specimens were prepared in different crystallographic orientations of the Si crystal by means of mechanical polishing and ion (Ar^+) beam thinning. Energy dispersive X-ray (EDX) spectrometry in the scanning transmission electron microscope (STEM) mode was used to measure the composition of the precipitates.

3 Results

3.1 *Cu precipitation in the voids*

Thermal annealing of the He-implanted silicon crystal causes the irradiation-induced point defects to form voids. The resulting layer of voids is shown in the plan-view TEM image in Fig. 1(a). The size of the voids ranges from a few nanometers to about 50 nm; such a wide range in void size distribution is useful for testing the dependence of the precipitation phenomenon on void dimension. The morphology of the voids, when viewed along the $[110]$ direction of the Si matrix (hereafter abbreviated as $[110]_{\text{Si}}$), shows facets mostly along $\{111\}$ planes in combination with $\{110\}$ and $\{100\}$ planes.

After application of the $\text{Cu}(\text{NO}_3)_2$ source the sample was heated to 850°C , immediately followed by slow cooling at a rate of 1 K/min. The slow cooling rate was set to ensure sufficient diffusion time for Cu to reach the voids and to avoid a rapid increase in the supersaturation of Cu. The result of the precipitation is shown in Fig. 1(b): about half of the voids are filled by the precipitates, and no partially filled void is observed. STEM EDX probing inside a

precipitate showed a stronger Cu signal than in the Si matrix, and the crystal structure of the precipitates was identified to be the hexagonal η' phase of Cu_3Si by TEM diffraction analysis [27], even though this is not the bulk equilibrium phase at room temperature. The η' phase has a hexagonal unit cell with space group $R\bar{3}$, and lattice parameters: $a = 35.16 \text{ \AA}$ and $c = 21.99 \text{ \AA}$. This phase has a constant orientation relation with the silicon matrix: $(0001)_{\eta'} \parallel (110)_{\text{Si}}; [11\bar{2}0]_{\eta'} \parallel [001]_{\text{Si}}$.

Results in samples annealed at different temperatures showed that the fraction of filled voids after precipitation increases with the annealing temperature, and hence with the equilibrium Cu concentration before precipitation. However, annealing above $850 \text{ }^\circ\text{C}$ or for a longer time did not raise the filled fraction to unity. A clean surface of a 1 cm^3 Si single crystal can accommodate all the interstitial Cu atoms dissolved in its lattice [14], so that part of the Cu atoms in the lattice may diffuse to the surfaces during cooling and leave an insufficient amount of Cu to fill all the voids. For this reason a 100 nm Cu layer was placed on the sample surfaces to saturate the surface sites by forming stable Cu silicide on the surface during annealing. Because the void walls are stronger traps for Cu than the Cu silicide phase [14], Cu precipitates preferentially at the void walls. The result after applying the surface Cu capping layer is shown in Fig. 1(c), in which all the voids are filled by the Cu_3Si precipitates after annealing at 800°C . This procedure was also tested for different annealing temperatures; the results showed that all the voids can be filled by Cu_3Si if the annealing temperature is between 500°C and 1000°C with a Cu capping layer on the surfaces. For example, in Fig. 1(d) all the voids are filled in a sample annealed at 500°C .

Figure 2 shows cross-sectional TEM micrographs of the precipitates in the Si matrix. The precipitates are located at the same depth as the empty voids, and no precipitates are observed at other depths. There are pronounced facets on the precipitate surfaces, which are parallel to $\text{Si}\{111\}$ planes. Together with the plan-view image of the precipitates in Fig. 1

(in $[100]_{Si}$ projection), which shows the rectangular facets of the precipitates parallel to $\langle 110 \rangle_{Si}$ directions, it appears that the precipitates are octahedra surrounded by eight $Si\{111\}$ planes with rounded corners. The uniform contrast of the precipitates in the TEM image indicates that they are single crystals, which is confirmed in the high-resolution TEM (HRTEM) image in Fig. 2(b). The lattice image of the precipitate consists of uniform Moiré fringes due to superposition of the precipitate and the Si lattice. The continuous and straight Moiré fringes in the precipitate are parallel to the $Si(111)$ plane, and they line up with the $Si(111)$ planes on the left edge. On the other side, the precipitate has a sharp interface parallel to the $Si(111)$ plane. Therefore, there is one set of lattice planes of the precipitate parallel to a $Si(111)$ plane. Measurement by TEM selected-area diffraction (SAD) shows that the spacing of these precipitate planes is 2.0 \AA , while the spacing of the parallel $Si(111)$ planes is 3.1355 \AA . This large difference in spacing makes an incoherent interface on the left edge of the precipitate. During coarsening of the precipitate, the growth rate of the incoherent edge is faster and the precipitate elongates in this direction, usually $\langle 111 \rangle_{Si}$, as can be seen in Fig. 2(a).

This precipitation process was also used in the voids created by annealing the 2 MeV He-implanted Si wafer. Figure 3 shows the precipitates in these voids after 900°C annealing and slow cooling. The position of the precipitates corresponds exactly to the location of original implantation-induced voids: most of the precipitates are located horizontally, Fig. 3(a), while precipitate clusters along the normal direction as in Fig. 3(b) are separated by a few micrometers. The Cu silicide precipitates in Fig. 3 have the same crystal structure, shape, and orientation as those discussed previously.

The results of Fig. 1 demonstrate no strong dependence of the precipitation behavior on the void size. The small voids in Fig. 1(a) are not present as precipitates after high temperature annealing; the number of small precipitates in Fig. 1(c) is much reduced from

that of the small voids in Fig. 1(a). On the contrary, small precipitates survive after low temperature precipitation, Fig. 1(d). Coarsening of the empty voids is a slow process: there is little change in void size distribution even after extensive annealing (1000°C for 1 h). Therefore, the possibility that the disappearance of the small voids after 850°C precipitation is due to prior coarsening of the voids can be ruled out. The average size of the precipitates in Fig. 1(c) is larger than that of the initial voids. Even though each precipitate is larger than the original void, for the reason that Si is consumed by its reaction with the arriving interstitial Cu to form Cu_3Si , this effect can not account for the large increase in precipitate size between Figs. 1(b) and 1(c). Thus, the increase in the average precipitate size in Fig. 1(c) is a result of the consumption of the small precipitates by Ostwald ripening.

Cu_3Si precipitates produced at a moderately fast cooling rate (~ 100 K/min) are shown in Fig. 4. Figure 4(a) shows that all the voids are nearly filled by the precipitates after fast cooling from 900°C, and that the size distribution of the precipitates is similar to that in Fig. 1(c): the density of small precipitates is still much lower than that of the small voids before precipitation. The large voids, however, are only partially filled by Cu_3Si precipitates, such that the unfilled volume attached to a precipitate is roughly proportional to the size of the precipitate. Precipitation by fast cooling from 600°C (Fig. 4(b)) produces a size distribution similar to that in Fig. 1(d), while small unfilled volumes are still present near the large precipitates and the small precipitates have not disappeared. Because the heating time for the samples in Fig. 4 is short, Cu_3Si precipitation in the voids appears to be a fast reaction with low activation energy. The nucleation rate of the silicides is probably independent of the void size, so that the small voids fill up while the large ones are still being filled. Further growth of the small precipitates is limited by the lattice strain energy. On the other hand, due to Gibbs-Thomson effect they tend to dissolve in favor of the large precipitates (coarsening). Coarsening of Cu_3Si precipitates need not overcome strain energy

in the Si lattice, nor generate extrinsic dislocation loops due to accumulation of the ejected Si interstitials. The ejected Si atoms during precipitate coarsening diffuse to the decomposed small precipitates that act as Si interstitial sinks; therefore, no extra volume is generated. It will be shown in the next section that dissolution is interface-reaction controlled, so that the coarsening phenomenon is more pronounced in high temperature precipitation.

The precipitation behavior does not change in the voids formed with H as the implanted species. Moreover, no difference was observed in high-purity intrinsic and p-type Si crystals, in which voids were created by implanting 2 MeV He ions. The cooling rate was kept slow to avoid homogeneous nucleation of precipitates due to a rapid increase in Cu supersaturation. However, if the concentration of the voids is much smaller than in the above 30 keV He-implanted samples, occasionally extra precipitation occurs in the shallow region between the crystal surface and a depth of a few micrometers, once all the voids are filled by the precipitates. For example, in the samples implanted by 2 MeV He⁺⁺ to a dose of $3.6 \times 10^{15}/\text{cm}^2$, the implanted area is small, so that the amount of Cu available for precipitation in each void is about an order of magnitude greater than in the He implanted sample in Fig. 1(a). Even with a slow cooling rate, the increased supersaturation thus led to the formation of precipitate colonies near the sample surface, especially in the implanted region that could contain defects caused by irradiation. The morphology of these precipitate colonies is similar to the reported heterogeneous growth of Cu silicide precipitates bounded by edge-type extrinsic dislocation loops [3, 4].

3.2 Stability of the precipitates against dissolution

Precipitates in the 2 MeV He-implanted samples, such as those in Fig. 3, were used to study their stability against dissolution. The surface-cleaned samples were made into TEM specimens and annealed in a furnace under flowing argon. The TEM results on the precipitates

before and after every anneal were used to investigate the degree of dissolution.

Two series of experiments were performed. In the first one, the specimen was annealed successively at 550°C for 6 h, 550°C for 24 h, and 700°C for 2 h. The results showed that the morphology of the precipitates did not change after each anneal. No dissolution of the precipitates was observed at these temperatures. The second specimen was annealed sequentially at 500°C for 22 h, 500°C for 6 h, 500°C for 6 h, and 850°C for 1 h. The specimen was examined after each anneal and the results after the last two anneals are shown in Fig. 5. The specimens were prepared to have the Si(111) plane parallel to the specimen surfaces, so that the width of the precipitate layer appears larger than in the [110] direction. Figure 5(a) shows that the precipitates are still complete after 34 h annealing at 500°C. The large void on the right side of the image appeared after the second 500°C annealing; the precipitate in this void was probably very near the surface of the specimen and dissolved easily. Subsequent annealing at 850°C for 1 h caused the precipitates to dissolve, as in Fig. 5(b). There are open volumes attached to most of the precipitates; self-interstitials apparently do not always fill the voids. Comparison between the positions of the precipitates in Figs. 5(a) and 5(b) shows that some of precipitates moved after dissolution as indicated by the arrows in Fig. 5(b), and have "tails" in the direction of their motion. The contrast change between the tails in Figs. 5(c) and 5(d), taken in opposite diffraction conditions for TEM imaging, shows that this dipole is bounded by two edge-type dislocations. A detailed contrast analysis showed that the dipole is a vacancy-type dislocation loop [28].

The formation of the vacancy-type dipoles can be explained by the mechanism described by Solberg and Nes: vacancies are emitted during dissolution of the Cu_3Si precipitates and aggregate to form dislocation dipoles [29]. In the TEM specimens, the Si crystal was thinned down to a thickness of a few hundred nanometers, so that the sample surface area per precipitate was much greater than that in the original wafer. The boundary condition for

dissolution changed from one limited by the solubility in the Si lattice to one of an infinite surface sink. Even in such a condition favorable to dissolution of precipitates, the rate of the dissolution is still low. This means that the dissolution is not diffusion- but interface-reaction controlled. The above results are consistent with those reported by McHugo *et al.* [30], in which the Cu silicide precipitates remain after a 560°C anneal for 45 min. They attributed the stability of their precipitates to the presence of oxygen, but the structure of our precipitates is the pure Cu₃Si phase.

The time for out-diffusion of interstitial Cu from a large sample used in the Avogadro project can be estimated as follows. Consider a silicon slab 1 cm wide with a mole fraction of Cu equal to 1.1×10^{-6} , the equilibrium solubility in silicon at 800°C. The clean surfaces of the silicon crystal act as perfect sinks for Cu atoms, so that the concentration of Cu at the surface is set at zero. A one-dimensional diffusion analysis [31] shows that the maximum Cu concentration in the silicon crystal drops to 2.6 ppb in 24 h if the out-diffusion experiment is performed at 500°C, at which the diffusivity of the interstitial Cu atom is 7.4×10^{-6} cm²/s [21]. The precipitates can stay stable at 500°C for more than 34 h. Therefore, the remaining Cu atoms after precipitation can be cleaned by low temperature out-diffusion without dissolution of the precipitates in the voids.

3.3 Precipitation of Ni, Au, and Fe in the voids

The heating condition for each metal was adjusted according to its physical properties, such as the diffusivity and equilibrium solubility in Si [21, 32]. Interstitial Ni, Au, and Fe atoms have low migration enthalpies and behave like Cu as fast diffusers in Si lattice, but, unlike Ni and Fe, a large fraction of Au dissolves substitutionally in silicon [21]. As a result, diffusion of Au is by the "kick-out" mechanism and takes a considerably more time to reach equilibrium throughout a Si crystal.

Ni was introduced into the silicon sample at 1000°C. Precipitates formed during cooling are typically larger than 100 nm, at the same depth as the original voids (see Fig. 6(a)), but their concentration is much lower than that of the voids. The SAD pattern in Fig. 6(b) contains clear diffraction spots from the precipitate's face-centered cubic (f.c.c.) structure along $[1\bar{1}0]$, and those of the surrounding silicon crystal along $[1\bar{1}0]_{Si}$, as schematically illustrated in Fig. 6(c). The f.c.c. diffraction pattern, the lattice plane spacings, as well as the composition measured in EDX show that the structure of the precipitate is NiSi₂, which has the cubic CaF₂ structure with a lattice parameter of 5.38 Å, about 1% smaller than that of silicon. Because the volume per silicon atom in the NiSi₂ structure is nearly the same as that in the silicon diamond cubic lattice, voids can never be filled by NiSi₂ precipitates. The precipitate in Fig. 6(a) must be the result of nucleation at a lattice defect.

Figure 7 shows the results of Au precipitation in the voids after annealing at 1000°C for 1 h followed by slow cooling. In the image not all of the voids are filled by the precipitates; the fraction of the filled voids can be increased by annealing for 10 h. This is consistent with the characteristic of Au diffusion in silicon: the U-shaped concentration profile through the thickness of a slab levels slowly with annealing time while the Au penetrates [21]. The precipitates in Fig. 7 consist of pure f.c.c. gold as determined from the SAD patterns. Precipitation of Au in the voids follows the simple eutectic reaction in the Au-Si phase diagram to form pure gold rather than a metastable Au silicide, which was formed by annealing a highly Au-supersaturated silicon single crystal followed by fast cooling [33]. There are two reasons that proscribe the use of Au to decorate the voids for the purpose of estimating the total volume of voids. First, the process is rather slow and takes much longer than for Cu to reach the equilibrium concentration inside a thick silicon crystal. Second, due to high substitutional solubility of Au in Si, out-diffusion of the Au atoms in the silicon crystal is difficult. As a result, the measured Au concentration in the Si crystal will not accurately

reflect the volume of the precipitates.

Fe did not form precipitates in the voids. Fe could be absorbed as a monolayer on the wall of the voids. To obtain the volume fraction of the voids in the Si crystal from the measured Fe content, a better understanding of the structure of the Fe monolayer is required. Furthermore, even with that knowledge, the determination of the volume fraction of voids is less straightforward than if the voids are filled entirely [20].

4 Discussion

The driving force for precipitation depends on the degree of supersaturation, and, hence, the precipitation mechanism varies with the cooling rate. If the cooling rate is low (<100 K/s), precipitate colonies bounded by extrinsic dislocation loops may form near the surface [3]. If the cooling rate is high (>1000 K/s), homogeneous precipitation accompanied by formation of stacking faults happens inside the Si crystal [11]. Therefore, slow cooling is preferred for Cu precipitation in the voids in order to avoid additional precipitates. However, as discussed in Sec. 3.1, precipitate colonies sometimes appear near the surface, even at a rate as slow as 1 K/min. This is probably the result of heterogeneous nucleation, for example at irradiation-induced dislocations. Existence of these extra precipitates is not a serious problem in the determination of the total void volume, because they are close to the surface and can be easily removed by either polishing or etching. Another option is to lower the annealing temperature to decrease the Cu concentration in the Si lattice before precipitation.

The first work on decorating silicon voids was carried out by Roksnoer and van der Boom [16]; they showed Cu-decorated voids (D-defects) in FZ Si ingots by X-ray topography. The microscopic structure of the precipitates and the direct link between the voids and the precipitates were not demonstrated. The concentration of the voids was estimated in lithium-decorated samples, and was shown to be positively correlated with the annealing

temperature toward a saturation value. Whether all the voids were decorated and revealed in the X-ray topography image was not conclusively determined. On the other hand, the results in Sec. 3.1 show directly that all the voids in a Si single crystal can be uniformly filled by the proposed Cu_3Si precipitation method.

The structure of the Cu precipitates has been suggested to be $\beta\text{-Cu}_{85}\text{Si}_{15}$ [9], which is stable at high temperatures, metastable hypothetical fcc-CuSi [4], and $\eta''\text{-Cu}_3\text{Si}$ [12]. Our work shows that the precipitate is the metastable η' phase [27]. Its structure, however, is still consistent with the early Cu silicide precipitation models [11, 13]. The η' phase consists of the hexagonal η unit cell, in which the volume per Si atom is 160% larger than that in the Si crystal. Thus, a large strain energy constraint is expected also for homogeneous nucleation of the $\eta'\text{-Cu}_3\text{Si}$ precipitates.

5 Conclusion

Voids in a Si single crystal can be completely filled by Cu_3Si precipitates if a Cu nitrate solution is used as a source and the surfaces of the sample are covered by Cu metal. Slow cooling (<100 K/s) prevents homogeneous nucleation of Cu silicide in the Si lattice. The stability of the precipitates allows low-temperature (500°C) out-diffusion of the remaining Cu atoms in solution. With the information from the crystal structure and composition, the conversion factor from the Cu content, from precise mass measurement, to the void volume fraction in the Si crystal can be obtained. The structure of the precipitates in the voids is the metastable hexagonal η' phase.

Acknowledgements

This work was supported by the National Science Foundation as a Cooperative Activity

in Materials Science between NSF and the European Commission. We are grateful for useful discussion with Joris Proost, and with Paul De Bièvre, Philip Taylor, Christophe Quétel and Vitas Aninkevicius of the Institute for Reference Materials and Measurements, a Joint Research Center of the European Commission.

References

- [1] W. C. Dash, *J. Appl. Phys.* **27** 1193 (1956).
- [2] L. Fiermans and J. Vennik, *Phys. Stat. Sol.* **12** 277 (1965).
- [3] E. Nes and J. Washburn, *J. Appl. Phys.* **42** 3562 (1971).
- [4] G. Das, *J. Appl. Phys.* **44** 4459 (1973).
- [5] H. J. Geipel and W. K. Tice, *Appl. Phys. Lett.* **30** 325 (1977).
- [6] H. Gottschalk, *Phys. Stat. Sol. A* **137** 447 (1993).
- [7] K. Ryoo, R. Drosd and W. Wood, *J. Appl. Phys.* **63** 4440 (1988).
- [8] M. Seibt, *Solid State Phenomena* **19&20** 45 (1991).
- [9] M. El Kajbaji, J. Dessus and J. Thibault, *Phil. Mag. A* **66** 873 (1992).
- [10] M. El Kajbaji and J. Thibault, *Phil. Mag. Lett.* **71** 335 (1995).
- [11] M. Seibt, M. Griess, A. A. Istratov, H. Hedemann, A. Sattler and W. Schröter, *Phys. Stat. Sol. A* **166** 171 (1998).
- [12] J. K. Solberg, *Acta Cryst. A* **34** 684 (1978).
- [13] E. Nes, *Acta Metall.* **22** 81 (1974).
- [14] S. M. Myers and D. M. Follstaedt, *J. Appl. Phys.* **79** 1337 (1996).
- [15] J. Wong-Leung, C. E. Ascheron, M. Petravac, R. G. Elliman and J. S. Williams, *Appl. Phys. Lett.* **66** 1231 (1995).
- [16] P. J. Roksnoer and M. M. B. van den Boom, *J. Cryst. Growth* **53** 563 (1981).
- [17] T. Sinno, E. Dornberger, W. von Ammon, R. A. Brown and F. Dupret, *Mater. Sci. Eng. R* **28** 149 (2000).
- [18] P. Becker, H. Bettin, H.-U. Danzebrink, M. Gläser, U. Kuetsgens, A. Nicolaus, D. Schiel,

- P. De Bièvre, S. Valkiers and P. Taylor, *Metrologia* **40** 271 (2003).
- [19] P. De Bièvre, S. Valkiers, R. Kessel, P. D. P. Taylor, P. Becker, H. Bettin, A. Peuto, S. Pettorruso, K. Fujii, A. Waseda, M. Tanaka, R. D. Deslattes, H. S. Peiser and M. J. Kenny, *IEEE Trans. Instrum. Meas.* **50** 593 (2001).
- [20] F. Spaepen and A. Eliat, *IEEE Trans. Instrum. Meas.* **48** 230 (1999).
- [21] W. Frank, U. Gösele, H. Mehrer and A. Seeger, in *Diffusion in Crystalline Solids*, edited by G. E. Murch and A. S. Nowick (Academic, New York, 1984), pp. 63-142.
- [22] C. Quétel, V. Aninkevicius, K. Filee and P. Taylor, Private communication.
- [23] S. M. Myers, D. M. Follstaedt and D. M. Bishop, *Mater. Res. Soc. Symp. Proc.* **316** 33 (1994).
- [24] J. Wong-Leung, E. Nygren and J. S. Williams, *Appl. Phys. Lett.* **67** 416 (1995).
- [25] B. Stritzker, M. Petravac, J. Wong-Leung and J. S. Williams, *Appl. Phys. Lett.* **78** 2682 (2001).
- [26] C. C. Griffioen, J. H. Evans, P. C. de Jong and A. van Veen, *Nucl. Inst. and Methods* **B27** 449 (1988).
- [27] C. Y. Wen and F. Spaepen, subsequent paper.
- [28] C. Y. Wen, *Precipitation of Copper Silicide in Voids in Silicon Single Crystals*. PhD thesis, Harvard University (2005).
- [29] J. K. Solberg and E. Nes, *Phil. Mag. A* **37** 465 (1978).
- [30] S. A. McHugo, A. Mohammed, A. C. Thompson, B. Lai and Z. Cai, *J. Appl. Phys.* **91** 6396 (2002).
- [31] J. Crank, in *The Mathematics of Diffusion* (Clarendon Press, Oxford, 1975).
- [32] E. R. Weber, *Appl. Phys. A* **30** 1 (1983).
- [33] F. H. Baumann and W. Schröter, *Phys. Rev. B* **43** 6510 (1991).
- [34] G. Weber, B. Gillot and P. Barret, *Phys. Stat. Sol. A* **75** 567 (1983).

Figure captions

Figure 1: (a) Plan view transmission electron microscope (TEM) image of implantation-induced voids in Si, seen along the $[001]$ zone axis. (b) Precipitation in the voids of a sample treated with $\text{Cu}(\text{NO}_3)_2$ after annealing at 850°C immediately followed by cooling at a rate of 1 K/min . (c) Precipitation with the application of an additional 100 nm Cu capping layer on the surfaces after annealing at 800°C followed by 1 K/min cooling. (d) Precipitates formed after a 500°C anneal for 30 min followed by slow cooling at a rate of 0.25 K/min .

Figure 2: (a) Cross-sectional TEM image along $[110]_{\text{Si}}$ of the precipitates. (b) High-resolution TEM image of a single crystalline precipitate in $[110]_{\text{Si}}$ projection.

Figure 3: Cross-sectional TEM images of the precipitation results in 2 MeV He-implantation-induced voids: (a) horizontal distribution of the precipitates; (b) distribution of the precipitates parallel to the implantation direction.

Figure 4: Plan view TEM images of the precipitates in the samples quenched from (a) 900°C and (b) 600°C .

Figure 5: (a) The precipitates annealed after their formation for 34 h at 500°C . (b) The precipitates in (a) after the sample has been further annealed at 850°C for 1 h . (c) The image of a partially dissolved precipitate (A) with a dislocation dipole (arrows) when $\mathbf{g}=[\bar{2}20]_{\text{Si}}$ is used for the bright-field image. (d) The dislocation contrast moves into the dipole when $\mathbf{g}=[2\bar{2}0]_{\text{Si}}$ is used for imaging.

Figure 6: (a) Cross-sectional TEM image of a NiSi₂ precipitate in the sample that was annealed at 1000°C after application of a Ni source followed by cooling at a rate of 1 K/min. (b) Selected-area diffraction (SAD) pattern of the precipitate. (c) A schematic illustration of the diffraction pattern.

Figure 7: Au precipitates in the voids after annealing at 1000°C after application of a Au source for 1h followed by cooling at a rate of 1 K/min.

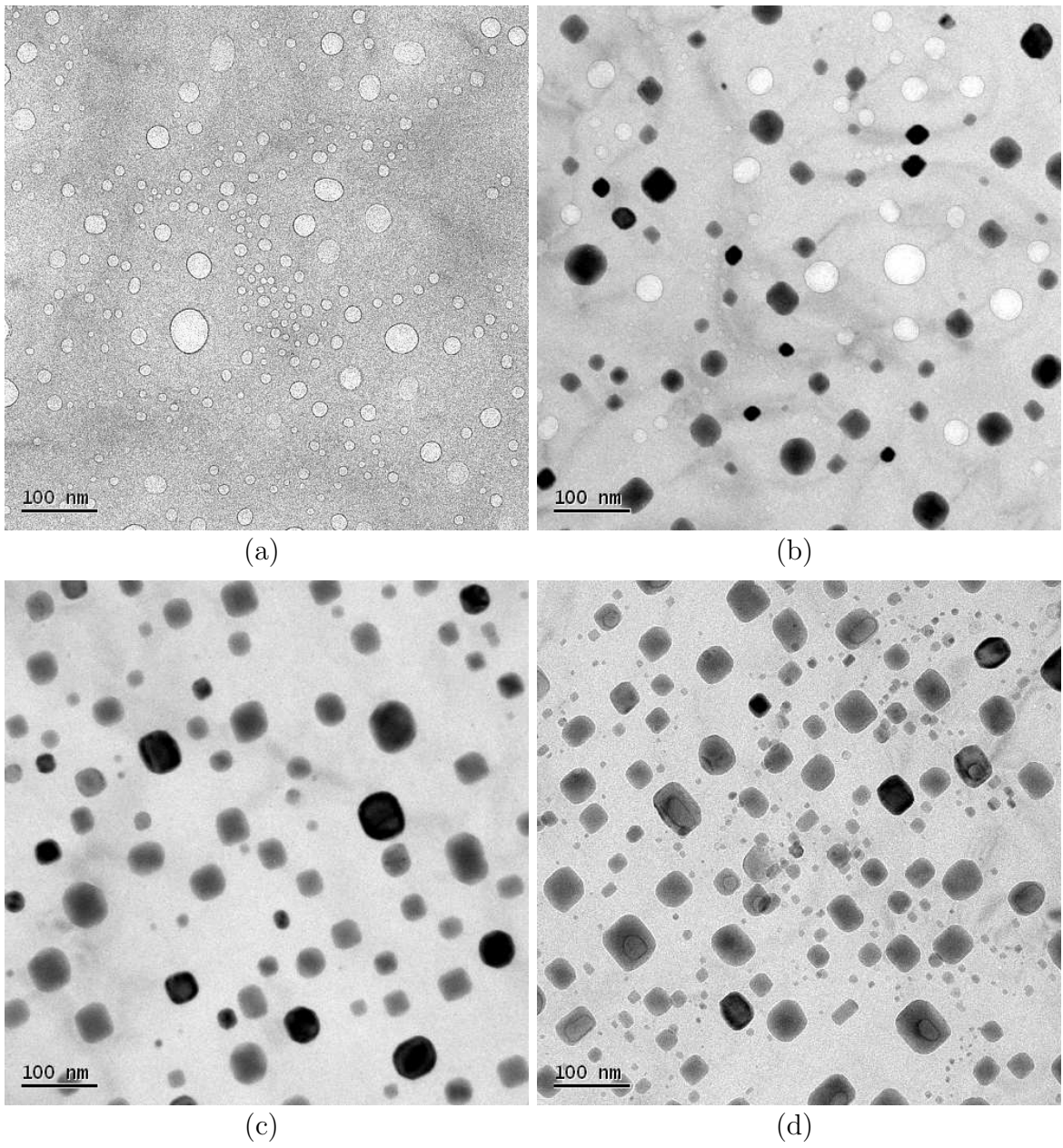
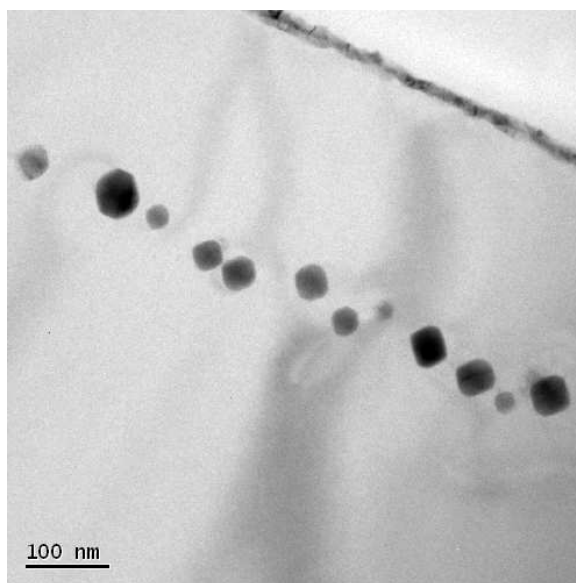
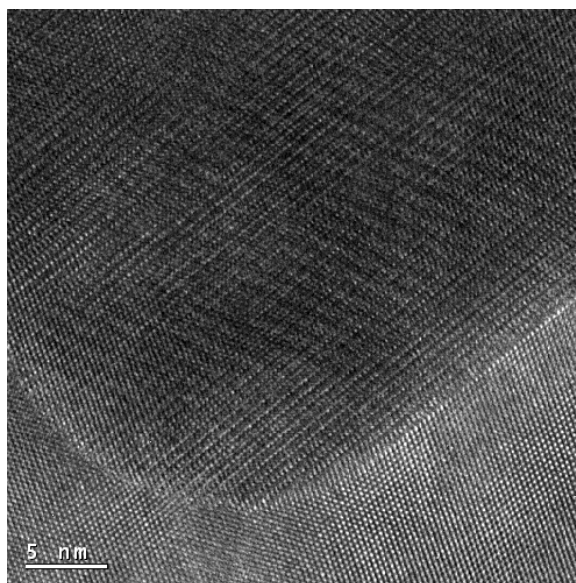


Figure 1.

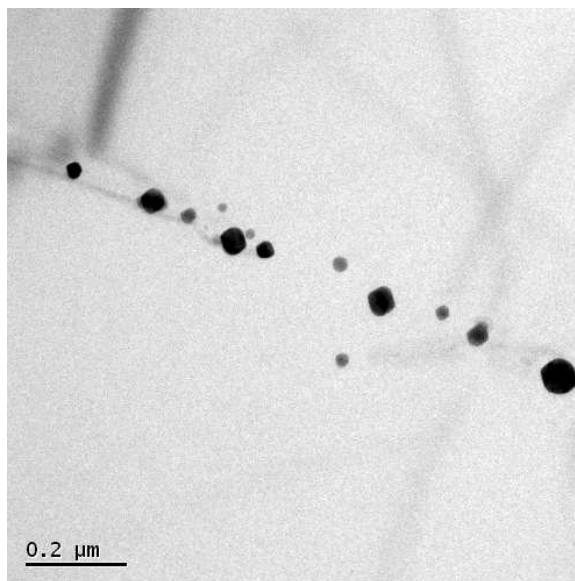


(a)

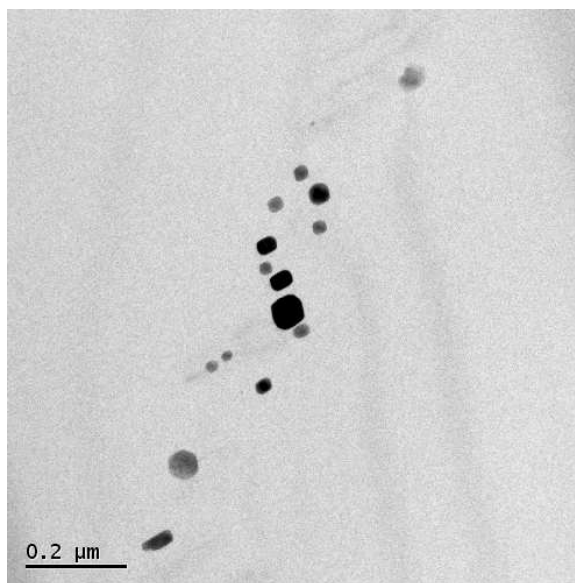


(b)

Figure 2.

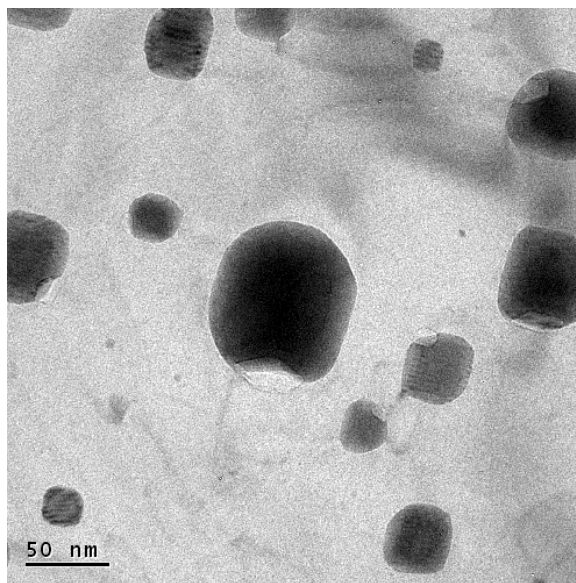


(a)

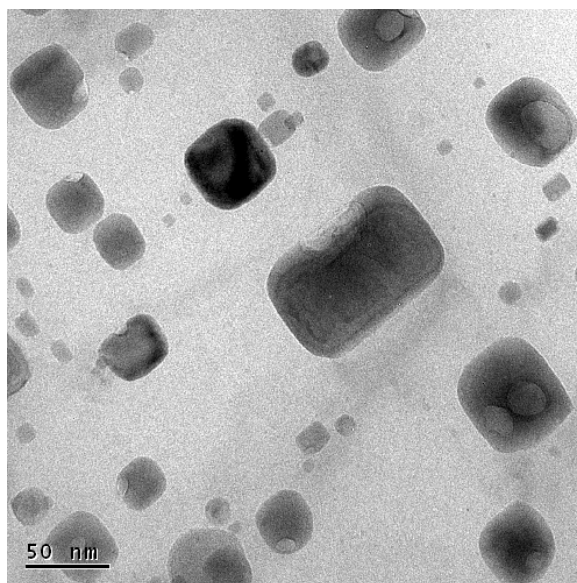


(b)

Figure 3.

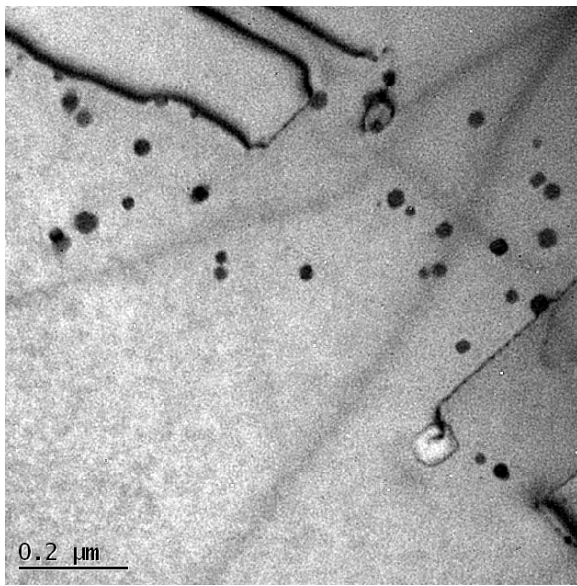


(a)

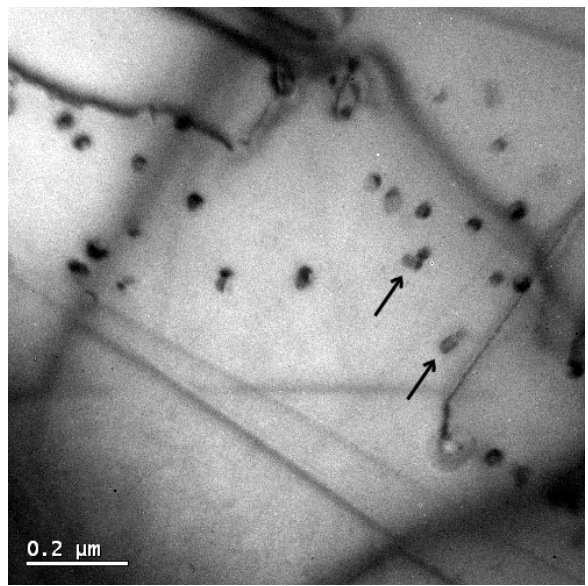


(b)

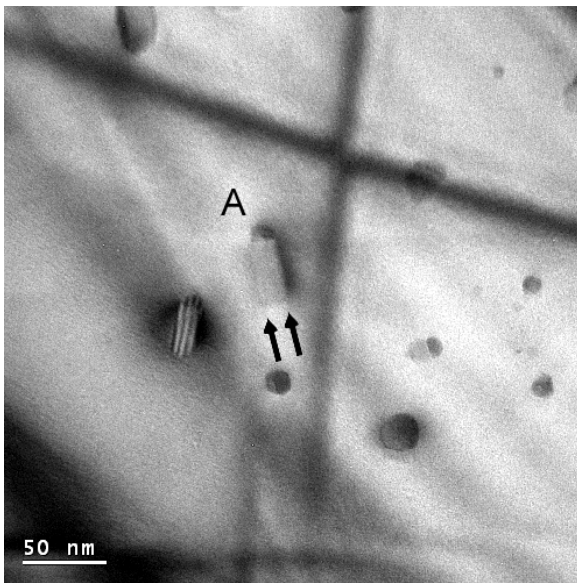
Figure 4.



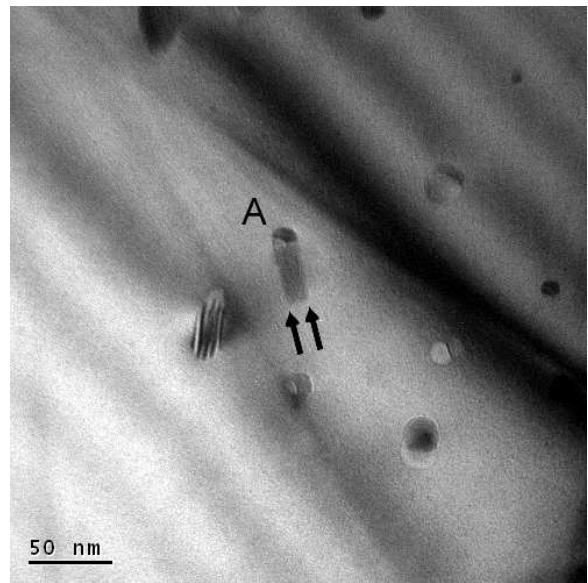
(a)



(b)

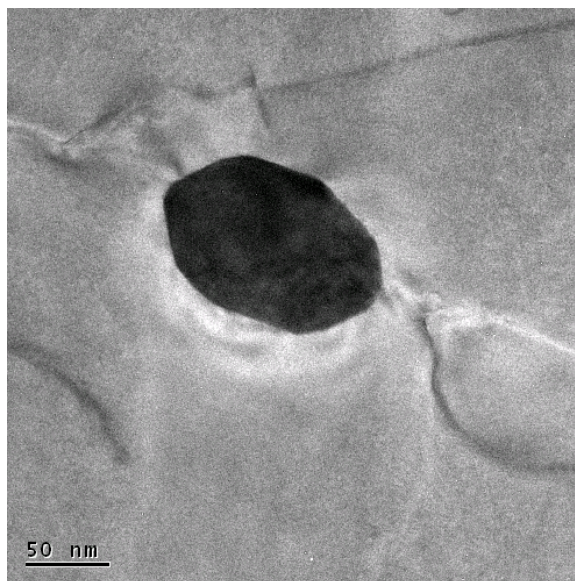


(c)



(d)

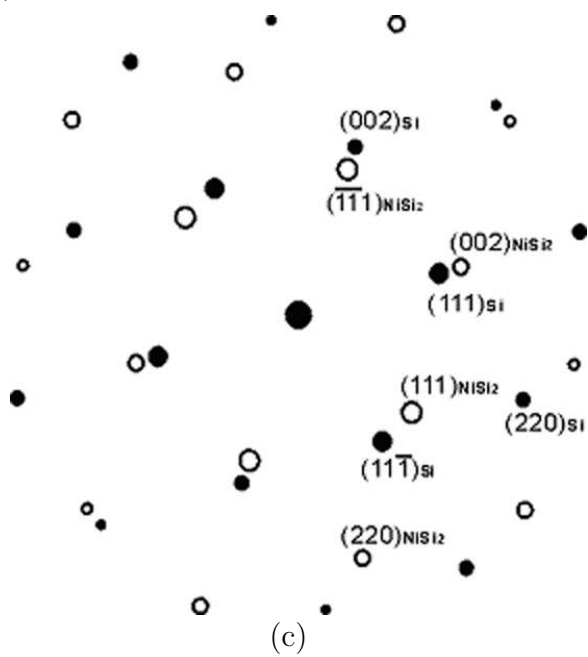
Figure 5.



(a)



(b)



(c)

Figure 6.

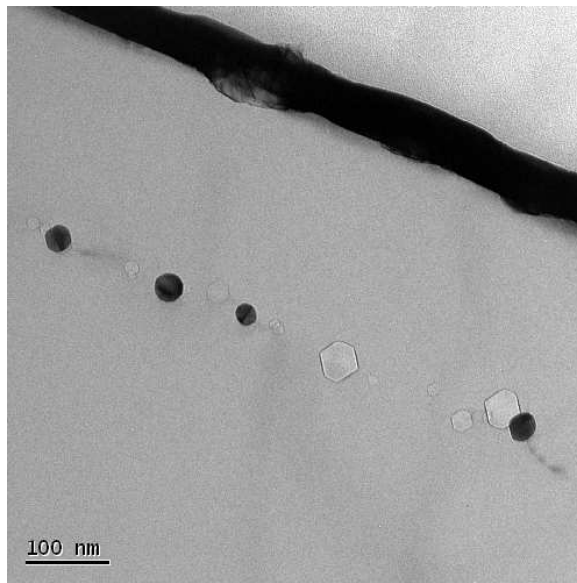


Figure 7.